CHAPTER 5

Laser Diode Characterization: Setup and Automation

5. Laser Diode Characterization: Setup and Automation

Fabrication of laser diode requires frequent testing during different stages of its evolution from structure-growth to packaging. The main characterizations include measurements of L-I characteristics, I-V characteristics, and spectral response. Further, the characteristic temperature, thermal impedance and lifetime are very important parameters for evaluation of laser diode performance. In order to maintain the uniformity of measurement conditions with higher precision and reliability, we have developed virtual instruments and established an automated laser diode characterization facility using LabVIEW. This chapter discusses the characterization setup along with interfacing and programming technology used for the automation.

5.1 Overview of Laser Diode Characterizations

It is often necessary to quantitatively evaluate the performance and characteristics of laser diodes. This is done through performing a series of experiments and obtaining certain significant parameters. Multiple characterizations are also necessary to optimize various processes for laser diode fabrication. Considering the increasing demand for laser diodes and the need of multiple testing stages, the speed and accuracy of testing are also the critical issues. The typical testing stages for a laser diode are shown in figure 5.1.

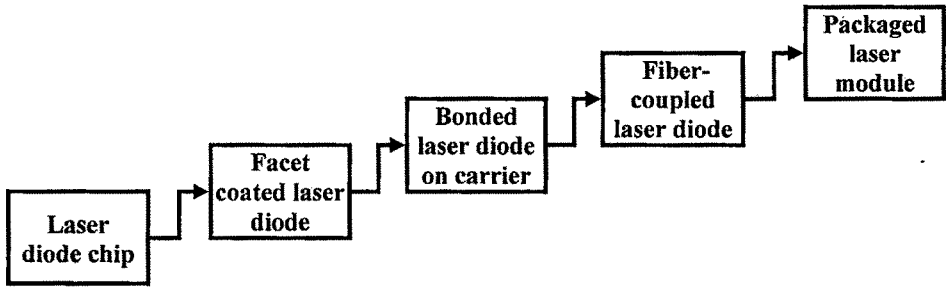

Figure 5.1: Laser diode testing stages.

The cost of testing and rejecting faulty laser diodes increases as one goes higher up the test stage. Measurement of light-current (L-I) characteristic and forward current-voltage (I-V) characteristic is an initial test of laser diode which can typically measure several key

parameters. L-I and I-V characteristics can also eliminate below-par lasers which could ultimately fail higher up the testing chain, where failure is more expensive. The spectral response measurement is also one of the fundamental characterizations for laser diode.

5.1.1 L-I Characteristics

The most important characteristic of a laser diode is the output light intensity versus input current curve, more commonly referred to as the L-I characteristic. Initially, the laser diode demonstrates spontaneous emission which increases very gradually with increasing current. After certain amount of current, the laser diode begins to emit stimulated radiation, which is the onset of laser action. A typical L-I curve of laser diode is shown in figure 5.2. Analyzing the L-I curve can yield some important information about the laser diode. The first parameter of interest is the exact current value at which the lasing starts. This is typically referred to as the threshold current and is denoted by the symbol I_{th}. Device efficiency and maximum power are the other important parameters that can be determined from the L-I curve.

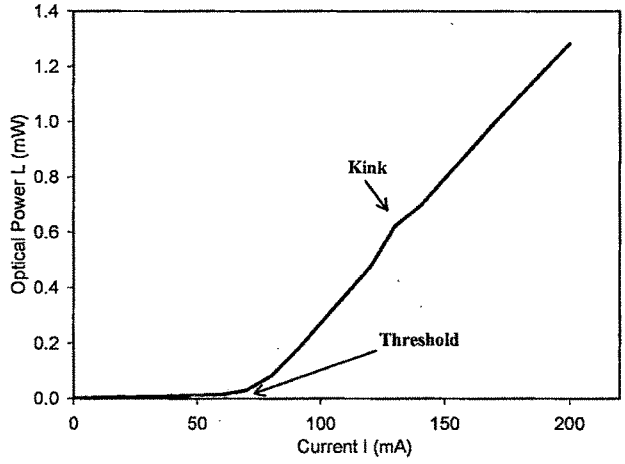

Figure 5.2: Typical L-I characteristic of laser diode.

5.1.1.1 Threshold Current

Threshold current is the current necessary for a laser diode to start the lasing. In other words, sufficient carriers must be supplied by means of current to compensate for losses, such as current leakage and nonradiative recombination processes, so that it can provide the necessary threshold gain. Spontaneous recombination dominates at a low current level

and the L-I curve (output power) remains low. Once the current level passes the threshold current, domination of stimulated emission causes a sudden rise in the slope of the curve, which indicates the beginning of lasing process [1].

Threshold current depends upon the quality of the semiconductor material from which the device is fabricated and the general design of the waveguide structure. However, the threshold current is more influenced by the physical dimensions of laser diode stripe, i.e., stripe width and cavity length. The threshold current is higher for a laser diode with larger stripe-area. Thus, it is better to evaluate the laser diode structures by means of threshold current density rather than by the threshold current. The threshold current density is the ratio of threshold current to stripe-area of the laser diode and is denoted by the symbol J_{th}. It is always desirable for a laser diode to have as low threshold current density as possible.

There are four different algorithms available to calculate the threshold current of a laser diode as shown in table 5.1 [2].

Table 5.1: Four methods of calculating threshold current.

Linear Fit	The point at which a straight line fit to the linear portion of L-I curve above the threshold intercepts the X-axis corresponding to the zero optical power
Two segment Fit	The point at which a straight line fit to the linear portion of L-I curve above the threshold intercepts the straight line fit to the linear portion of the curve below it
First Derivative of L-I	The point at one half the maximum of the rising edge of the dL/dI curve
Second Derivative of L-I	The point at which the dL/dI curve is maximum

We have combined the Linear Fit method with the Second derivative method to find the threshold current programmatically from experimental L-I curve.

5.1.1.2 Slope Efficiency

A laser diode should also exhibit a good conversion rate of input electrical power to output optical power. A direct measure of the conversion rate of laser diode is the slope of the L-I curve above the threshold current, called slope efficiency. It is denoted as dP/dI and has the units of Watts per Amperes (W/A). The slope efficiency of the laser diode should ideally be a constant above threshold up to a saturation point and can be obtained by differentiating the L-I curve above threshold. A typical differentiated L-I characteristic is shown in figure 5.3 [a]. The further differentiation of this data gives threshold current and other kinks in the form of peaks as shown in figure 5.3 [b].

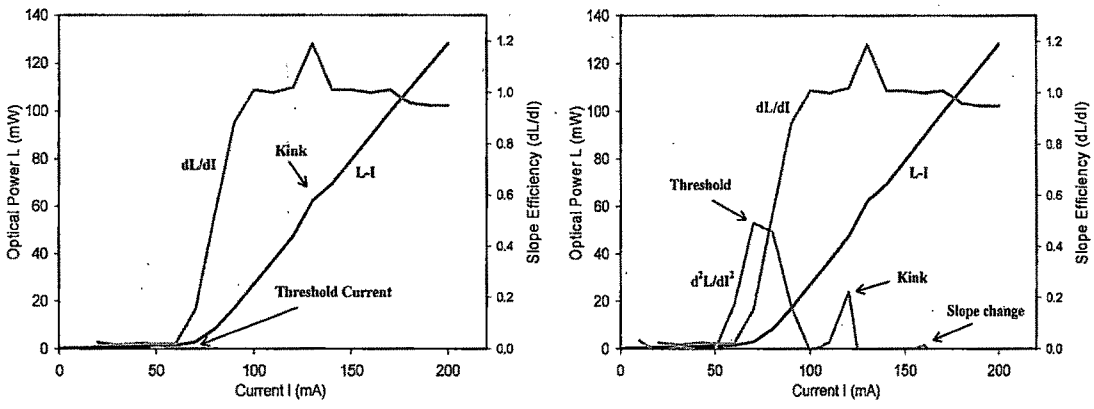

Figure 5.3: [a] First and [b] second differentiation of L-I characteristics.

5.1.1.3 External Differential Quantum Efficiency

External differential quantum efficiency, η_D [3] is another parameter that can directly be extracted from the L-I characteristic of laser diode. This is a figure of merit, measured in percentage, which indicates the efficiency of a laser diode in converting the injected electron-hole pairs to photons emitted from the diode. In an ideal laser diode, the recombination of each electron-hole pair results in the emission of one photon. In a real laser diode, however, the recombination of some electron-hole pairs result in the generation of other, undesirable, forms of energy, such as heat. Moreover, not all the photons generated inside the cavity are emitted from the laser diode. Some of them are reabsorbed within the waveguide structure.

Thus, on increasing current I by an amount dI, i.e., by injecting dI/q numbers of charge carriers in time dt, where q is the fundamental electronic charge, if the optical power increases by an amount dP, then we get dP/(hc/λ) number of photons emitted out, where (hc/λ) is the energy of single photon with wavelength λ. Thus, according to the definition of external differential quantum efficiency,

$$\eta_D = \frac{dP/(hc/\lambda)}{dI/q} = \frac{q\lambda}{hc}\frac{dP}{dI} \tag{5.1}$$

where, h is the Planck's constant, c is the velocity of light in vacuum and dP/dI is the slop efficiency of the laser diode.

5.1.1.4 Kinks

Evidence of undesirable "kinks" or non-linearities in the L-I curve point to the inherent problems that will mean rejection of the device. For example a kink can be indicative of filamentary emission due to defects in laser structure or mode-hopping in the optical spectrum [4], which is very undesirable, particularly in applications like optical pumping and optical communication [5].

Furthermore, by varying the measurement conditions for L-I characteristics, more important parameters like characteristic temperature T_0 and thermal impedance R_{th} of laser diode can be extracted. The characteristic temperature of laser diode can be obtained by measuring L-I characteristic at different temperature and is discussed in detail in section 5.5.2. By measuring L-I characteristics in pulsed and continuous-wave (CW) mode allows to determine the thermal impedance of laser diode and is described in section 5.5.3

5.1.2 I-V Characteristics

I-V characteristic is also an important measurement for laser diode, just as in case of any other electronic and optoelectronic device. A typical I-V characteristic of a laser diode is shown in figure 5.4.

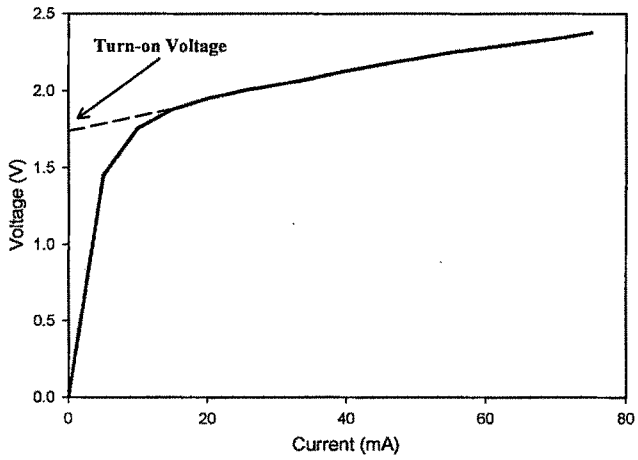

Figure 5.4: Typical I-V characteristic of laser diode.

The series resistance of the laser diode is typically determined form the slope of the I-V characteristic curve above the turn-on voltage [6]. High series resistance values could be a leading factor in the degradation of laser diode. Turn-on voltage is another parameter that can be obtained from I-V curve and is an indication of the lasing wavelength of laser diode.

5.1.3 Spectral Response Measurement

Most conventional gain or index guided devices have a spectrum with multiple peaks and are multi-mode lasers. The number of spectral lines supported by a laser diode depends upon the cavity structure [7]. The optical wave propagating through the laser cavity forms a standing wave between the two mirror facets of the laser diode. The period of oscillation of this curve is determined by the distance L between the two mirrors. This standing optical wave resonates only when the cavity length L is an integer number m of half wavelengths existing between the two mirrors, i.e., for $L = m\lambda/2$, where λ is the wavelength of light in the semiconductor material and is related to the wavelength of light in free space λ_0 through the index of refraction n by the relationship $\lambda = \lambda_0/n$. As a result of this situation, there can exist many longitudinal modes in the cavity of the laser diode each resonating at its distinct wavelength of $\lambda_m = 2L/m$. Thus, a multi-mode laser diode exhibits spectral output having many peaks around their center wavelength. The two adjacent longitudinal laser modes are separated by a wavelength of $\Delta\lambda = (\lambda_0)^2 / 2nL$. Unlike the multi-mode laser diodes, single frequency laser diodes such as Distributed

Feed-Back (DFB) and Distributed Bragg Reflector (DBR) type of devices display a single well defined spectral peak [8,9]. Figure 5.5 shows these two spectral behaviors.

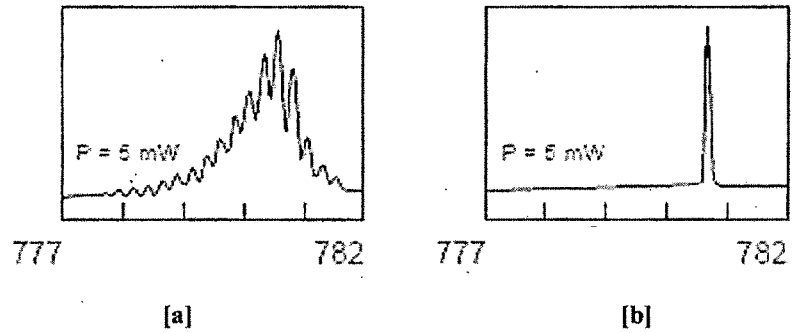

[a] [b]

Figure 5.5: Typical spectral response of [a] multi-mode and [b] single-mode laser diode.

The lasing wavelength strongly depends on the operating temperature of laser diode [10]. As the temperature increases, the center wavelength shows the red-shift. This property of laser diode is useful in optical communication [11,12], spectroscopic applications [13,14], and pumping of solid state lasers [15] where the emission-wavelength of the laser diode can be accurately temperature-tuned.

5.2 Instruments for Laser Diode Characterization

The laser diode characterization requires various sophisticated equipments. The laser diode is driven with the help of a current driver. The optical power is measured using a photodetector, an integrated sphere and a lock-in amplifier. The laser diode is mounted on a thermoelectric cooler (TEC) based temperature controller with heat sink arrangement. The spectral response measurement is carried out using a monochromator. The main instruments used for laser diode characterization are briefly described below.

5.2.1 Current Driver

A precise laser diode current source is critical for L-I and I-V characteristics measurements. Any good laser diode current source must both drive and protect the laser diode under test. Protection means that external current and voltage spikes must not reach the laser diode. The ability to pulse a laser diode at low-duty-cycles is very useful in

diode evaluation since a laser diode will not generate significant heat in a pulsed manner and the characterization can be accomplished with minimal thermal effects.

We have used ILX Lightwave's LDP-3840 Precision Pulsed Current Source for low power pulsed measurements of laser diodes. LDP-3840 is a microprocessor controlled instrument ideal for providing clean, reliable current pulses to laser diodes. The driver provides 0 to 3 Amp maximum peak pulse current, with pulse widths adjustment from 100 ns to 10 μs. The advanced pulse network of the LDP-3840 provides fast rise times while maintaining overshoots less than 5%, and offers selectable polarity pulse modes.

For high-power and CW operation, we have used Newport-5600 high-power laser diode driver. The driver is capable to source up to 65 A CW current with high precision. It can also be operated in quasi-CW (QCW) mode with 0.25% to 20% duty cycle variation. The pulse width can be varied from 100 μs to 1 s. The driver also has the facility to measure the forward voltage across the diode as well as the optical power through photodetector or thermopile detector directly.

5.2.2 Integrating Sphere

Integrating spheres are designed to collect the power of highly divergent laser beams from laser diode or other light sources, since these beams can overfill the input of a photodetector and cause considerable measurement error. The hollow spherical cavity has a diffusive internal wall and two or more ports. The photodetector placed on one port measures the light intensity and depending on the integrating sphere's attenuation and calibration data, the optical power can be measured. The optical power measurement with integrated sphere is insensitive to errors caused by the detector positioning or problems associated with overfilling or saturation of the active area of detector.

Typically the laser diode is positioned very close to the internal port of the sphere as shown in the figure 5.6 and light emitted from the front facet of the device is collected by the internal cavity of the integrating sphere which is coated with a highly reflective material. A baffle positioned between the input port and the detector port prevents the

detector from directly viewing the emitting aperture of the laser. What the detector sees is a uniformly illuminated environment within the cavity of the sphere.

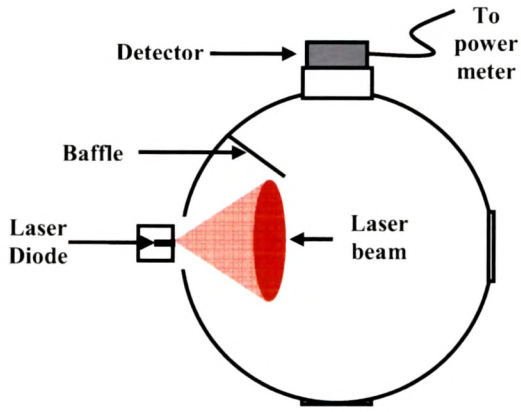

Figure 5.6: Schematic representation of integrating sphere.

In an integrating sphere, the detected radiation flux is always a small fraction of the incident flux. This attenuation caused by light reflecting many times before reaching the detector makes the integrating sphere an ideal tool for measurement of optical output power of high-power laser diodes. We have used Newport's 819-IS-2 inch integrating sphere which is suitable for laser diode measurements because of their relatively thin walls, only a few millimeters thick, making it possible to position the laser diode very close to the internal cavity of the sphere. Figure 5.7 shows the actual photograph of the integrating sphere used for the experiments with a photodetector fixed on one of its ports. The assembly consists of a Model 819-IS integrating sphere with one of the 818 Series low-power semiconductor detectors, and is calibrated to NIST traceable standards.

Figure 5.7: Photograph of integrating sphere with photodetector.

5.2.3 Photodetector

The photodetector senses the optical power of the light falling upon it and converts the variation of this optical power into a correspondingly varying photo-current. Among the foremost of these requirements is a high response or sensitivity in the emission wavelength range of the optical source being used, a minimum addition of noise to system and a fast response speed or sufficient bandwidth to handle the desired data rate. The photodetector should also be as insensitive to variations in temperature as possible and have a long operation life.

The choice of the detector depends on the wavelength of emission of the laser diode. A variety of semiconductor detectors are available to cover the spectral range from 200 – 1800 nm. The responsivity range of a photodetector is principally determined by the construction of the detector and the type of material used. We have used the 818 Series low power semiconductor detectors for laser diode characterization setups. For wavelength range from 400 nm to 1100 nm, Model 818-SL silicon detector is used while from 1100 nm to 1800 nm wavelength range, 818-IR germanium detector is used for the experiments in combination with the integrated sphere. For high-power laser diodes, optical attenuators are used in front of photodetectors. Figure 5.8 shows the photograph of two photodetectors used for the experiments.

Figure 5.8: Photograph of photodetectors used for the experiment.

5.2.4 Lock-in Amplifier

Operation and significance of a lock-in amplifier can be visualized in a number of ways. The lock-in amplifier relies on the concept of phase sensitive detection [16]. The Phase

sensitive detection refers to the demodulation or rectification of an ac signal by a circuit which is controlled by a reference waveform. The phase sensitive detector effectively responds to signals which are coherent (same frequency and phase) with the reference waveform and rejects all others. In a light measurement system the device which causes the signal to be modulated is usually a chopper or pulsed current driver. The reference waveform is an output coherent with the chopping action provided by the chopper or trigger pulses from current driver and the ac signal is the signal from the photo detector.

An approach to visualizing the phase sensitive detector is to consider the switch as a multiplier as shown in figure 5.9.

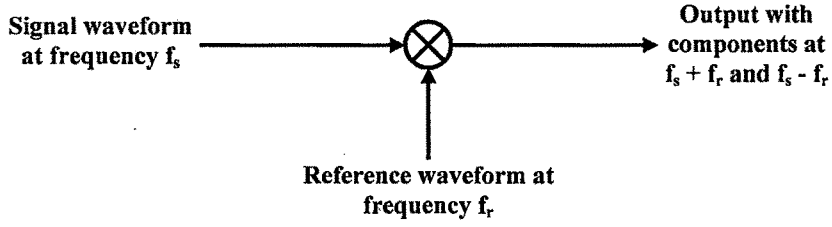

Figure 5.9: Simplified view of lock-in operation.

The output of a multiplier switch includes component at two frequencies, $f_s + f_r$ and $f_s - f_r$. If $f_s = f_r$, as is the case where the reference waveform is derived from the device which is modulating the signal, then there will be an output at 0 Hz i.e. dc. Any other component in the signal e.g. a noise component at a frequency of f_n will give rise to an ac output at frequencies of $f_n + f_r$ and $f_n - f_r$ which will be smoothed or averaged to the mean value of noise, i.e. zero, by the filter.

Lock-in amplifiers are used to detect and measure very small AC signals – all the way down to a few nano-volts. Accurate measurements may be made even when the small signal is obscured by noise sources thousands of times larger. The device behaves as a band pass filter and performs the same function as a tuned amplifier followed by a rectifier but with some advantages like a very precise bandwidth and very high noise rejecting capability. We have used SR-530 analog lock-in amplifier supplied by Stanford Research Systems, Inc.

5.2.5 Temperature Controller

The operating temperature of laser diode in our experiments was controlled by means of a combination of a TEC, and a feedback temperature monitor semiconductor IC (LM 35). The temperature is controlled programmatically with the help of LabVIEW. Temperature test range possible in our setup was from 0 °C to 60 °C.

5.2.6 Monochromator

The monochromator is very useful instrument in spectroscopic characterizations. It passes only a certain desired wavelength of light with a small band-pass window from a polychromatic input light. It is based on diffraction of light by a grating. One or more diffraction gratings are mounted on a stepper motor and can be rotated to get desired wavelength diffracted at the output slit. The band pass is determined by the slit width. We have used CVI's CM-110 1/8 m monochromator for spectral response measurement of laser diodes. The monochromator contains two gratings, one with 600 groves/mm and the other with 1200 groves/mm. The two grating cover wide spectral range from 0 to 3000 nm with the resolution of 0.2 nm.

5.3 Automation of Characterization Facility

In order to carry out laser diode characterization in less amount of time with better accuracy and uniformity, we have automated the whole laser diode characterization facility. The automated characterization facility allows very fast data acquisition with more precision and reliability. Since the test and measurements are done in a very less time, there is a reduced chance of device failure even for bad devices. Moreover, it eliminates the human errors in measurements. Since the data are acquired directly in to the PC, quick mathematical calculations, easy data processing and analysis are possible. We have followed the virtual instrumentation approach for the automation of laser diode characterization facility.

5.4 Virtual Instrumentation

Virtual Instrumentation is the use of customizable software and modular measurement hardware to create user-defined measurement systems, called virtual-instruments (VIs) [17]. Conventional instrumentation systems are made up of pre-defined hardware components, such as digital multimeters and oscilloscopes that are completely specific to their measurement or analysis function. Because of their hard-coded functionalities, these systems are more limited in their versatility than virtual instrumentation systems. The primary difference between conventional instrumentation and virtual instrumentation is the software component of a VI. The software enables complex and expensive equipment to be replaced by simpler and less expensive hardware. Thus, a VI is a user defined and user designed instrument that brings all the necessary equipments for an experiment on a single workbench. The VI provides great functional flexibility to the user. Moreover, since VI is a PC based instrument, the data acquisition, analysis, and presentation of results are all done together on a single platform.

The Virtual instrumentation involves three technologies and, in general, allows the user to use the PC as a flexible instrument for measurements and characterization. These are:

1. Data Acquisition System
2. Communication protocols
3. Programming

5.4.1 Data Acquisition System

The Data Acquisition (DAQ) System consists of the PC and other hard wares to make the physical component of the VI. The elements of the DAQ system include the PC, transducers, signal conditioning, DAQ hardware and software as shown in figure 5.10.

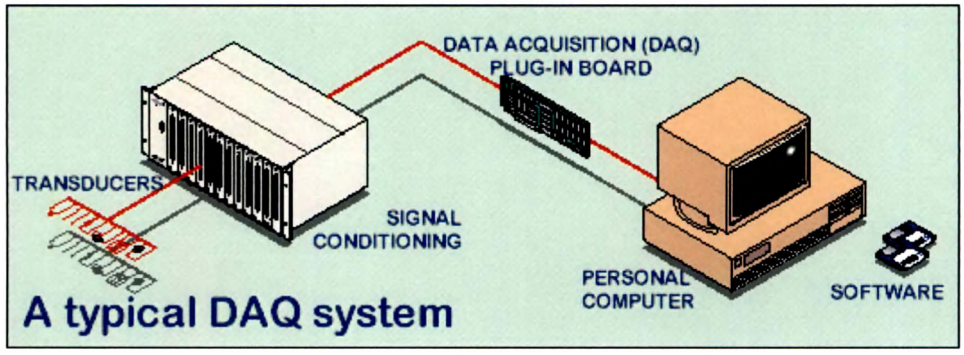

Figure 5.10: A typical data acquisition system.

5.4.1.1 The Personal Computer

The PC is a main platform for the user to acquire, analyze and present the data in appropriate manner. The PC used for the data acquisition system decides the maximum speeds at which one can continuously acquire the data. However, for remote data acquisition applications that use RS-232 or RS-485 serial communication, the data throughput will usually be limited by the serial communication rates.

5.4.1.2 Transducers

Transducers sense physical phenomena and provide electrical signals corresponding to the physical quantity. For example, thermocouples, resistance temperature detectors (RTDs), thermistors, and IC sensors convert temperature into an analog signal that an ADC can handle. Other examples include strain gauges and photodetectors, which measure force and light intensity respectively. In each case, the electrical signals produced are proportional to the physical parameters they are monitoring.

5.4.1.3 Signal Conditioning

The electrical signals generated by the transducers must be optimized for the input range of the DAQ board. Signal conditioning accessories can amplify low-level signals, and then isolate and filter them for more accurate measurements. In addition, some transducers require voltage or current excitation to generate a voltage output which can be provided by the signal conditioning circuit.

5.4.1.4 DAQ hardware

The DAQ hardwares, which are usually special kind of circuit boards, are generally installed in the PC. These hardwares convert the electrical signals conditioned by the signal conditioners into the data format which can be understood by the PC. We have used National Instrument's PCI-6024E DAQ card in combination with BNC-2120 connector block for our data acquisition purpose. The details about the DAQ card and connector block are as below.

❖ PCI-6024 Data Acquisition Card

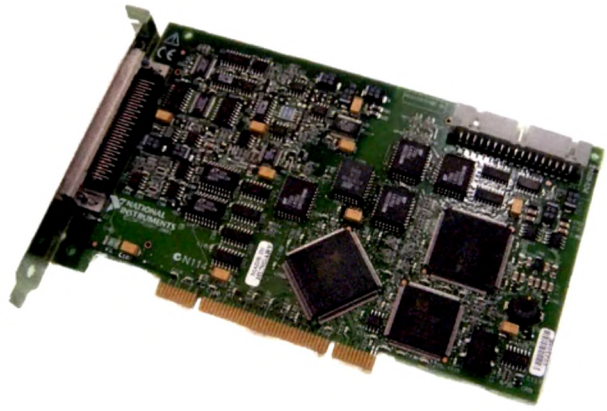

Figure 5.11: PCI-6024E data acquisition card.

The National Instruments PCI-6024E is a low-cost data acquisition board that delivers high-performance, reliable data-acquisition capabilities in a wide range of applications. It provides 12-bit resolution on 16 single-ended analog inputs with sampling rate up to 200 kS/s and two 12-bit analog outputs with sampling rate of 10 kS/s. It also contains 8 digital I/O lines and two 24-bit counters. The input and output voltage range is from -10 V to +10 V.

❖ BNC-2120 Connector Block

The BNC-2120 is a desktop or DIN rail-mountable accessory. The BNC-2120 has eight BNC connectors for analog input (AI) connection with a thermocouple connector, a

temperature reference, and resistor measurement screw terminals. Two BNC connectors are available for analog output (AO) connection. Moreover, screw terminals are given for digital input/output (DIO) connection with state indicators. In addition, it contains two user-defined BNC connectors and a function generator with a frequency-adjustable, TTL-compatible square wave, and a frequency- and amplitude-adjustable sine wave or triangle wave and a quadrature encoder. The BNC-2120 is connected directly to the PCI-6024E DAQ card through a 68-pin input/output (I/O) port available on BNC-2120. Figure 5.12 [a] shows the block diagram of BNC-2120 front panel. The actual photograph of the connector block is shown in figure 5.12 [b].

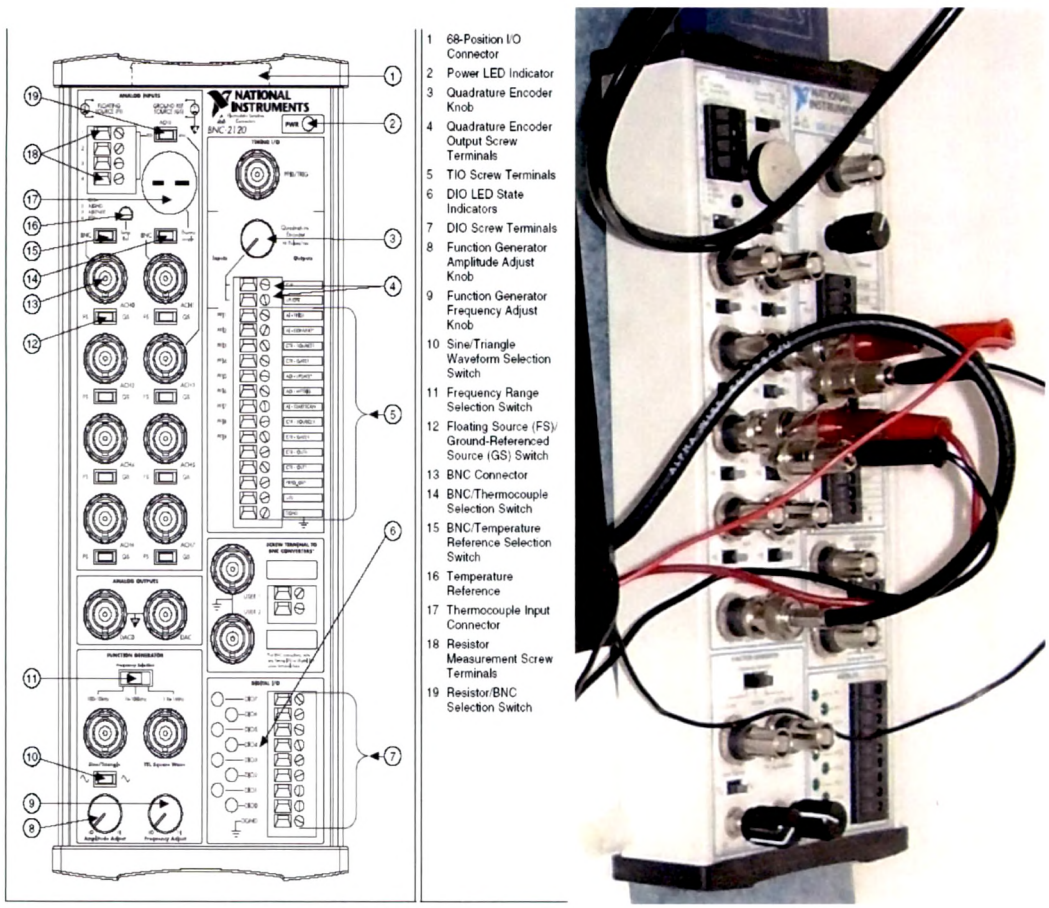

Figure 5.12: BNC-2120 [a] block diagram of front panel and [b] actual photograph.

However, in many applications, a digital signal generated by the signal conditioner can directly be fed to the PC through parallel port, serial port or other kind of interfacing board like GPIB.

5.4.1.5 Software

Finally, the signals in the form of digital data are processed in the PC with the help of appropriate software and are analyzed to give meaningful information about the device under test (DUT). We have used National Instrument's LabVIEW as a software tool to build our VIs. Details about the LabVIEW software are given in section 5.4.3

Figure 5.13 shows a complete DAQ system developed at our laboratory for semiconductor junction characterization. Here, a temperature sensor IC, 'a', works as a transducer that converts temperature into the electrical signals and feed to the DAQ hardware through a signal conditioning device, a buffer 'b'. The buffer isolates the DUT and PC, and allows safe I-V measurements. The control signal and measured data are handled by means of a DAQ card PCI-6024E (not visible in picture), installed in the PC, through a BNC connector block, BNC-2120, 'c', as shown in figure 5.13.

Figure 5.13: A DAQ system developed at our laboratory for semiconductor junction characterization.

5.4.2 Communication Protocols

A typical laboratory setup will use multiple instruments to conduct an experiment. For a virtual instrumentation, any of these or all instruments need to be connected to the PC. There are various communication protocols to connect different hardwares and instruments with PC. These protocols include serial communication, parallel communication, general purpose interface bus (GPIB), VXI, etc.

5.4.2.1 Serial Communication

Serial communication is a popular means of transmitting data between a computer and a peripheral device such as a programmable instrument or even another computer. Serial communication uses a transmitter to send data, one bit at a time, over a single communication line to a receiver. One can use this method when data transfer rates are low or one must transfer data over long distances.

For serial communication, four parameters have to be specified: baud rate of the transmission, number of data bits encoding a character, parity bit (optional), and number of stop bits. Each transmitted character is packaged in a character frame, which consists of a single start bit followed by the data bits, the optional parity bit, and the stop bit or bits. The figure 5.14 shows a typical character frame encoding the letter 'm'.

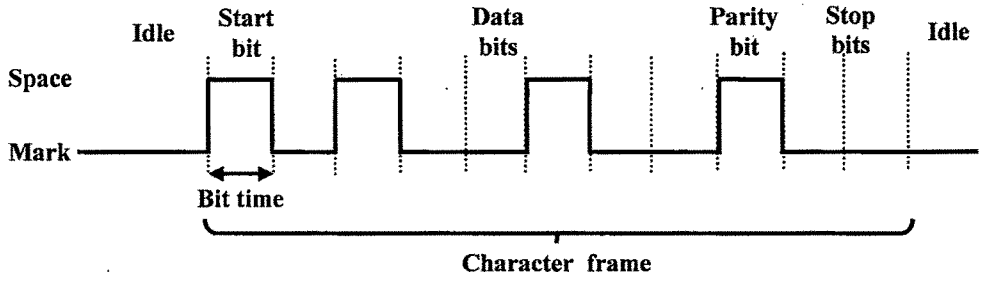

Figure 5.14: A package of a single byte containing data and framing bits.

Serial Ports can be of two types, D-Type 25 pin connector and D-Type 9 pin connector. There are different standards of serial port communication, including RS-232, RS-449, RS-422, and RS-423. RS-232 is the most widely used serial communication standard.

5.4.2.2 Parallel Port Communication

The Parallel Port allows the input of up to 9 bits or the output of 12 bits at any given time, thus requiring minimal external circuitry to implement many simpler tasks. The port is composed of 4 control lines, 5 status lines and 8 data lines. It uses mostly a D-Type 25 Pin female connector. Newer Parallel Port's are standardized under the IEEE 1284 standard first released in 1994.

5.4.2.3 GPIB

The GPIB, also commonly referred to as IEEE 488 or HPIB, was invented by Hewlett-Packard Corporation in 1974 to simplify the interconnection of test instruments with computers [18]. It is a digital, 8-bit parallel communications interface with data transfer rates of 1 Mbyte/s and higher, using a three-wire handshake. A standard GPIB setup has one controller, one or more instruments and GPIB cables.

Figure 5.15: National Instruments' PCI-GPIB board with GPIB cable.

The controller usually refers to a PCI-GPIB board connected to a PC. The picture of GPIB board used for the experiment is shown in figure 5.15. This controller allows the user to interact with the instruments. The instrument can be anything that has a GPIB connection such as current driver, lock-in amplifier, etc. The GPIB cable simply connects

the instrument and the controller. These instruments can either be arranged in a star configuration as shown in figure 5.16 [a] or in a linear configuration as in figure 5.16 [b].

[a] [b]

Figure 5.16: [a] Star configuration and [b] linear configuration for GPIB interfacing.

The GPIB uses a 24-conductor parallel bus that consists of eight data lines, five bus management lines (ATN, EOI, IFC, REN, and SRQ), three handshake lines, and eight ground lines. GPIB uses a byte-serial, asynchronous data transfer scheme. This means that whole bytes are sequentially handshake across the bus at a speed that the slowest participant in the transfer determines. Because the unit of data on the GPIB is a byte (eight bits), the messages transferred are frequently encoded as ASCII character strings. All GPIB devices and interfaces must have a unique GPIB address between 0 and 30. Address 0 is normally assigned to the GPIB interface. The instruments on the GPIB can use addresses 1 to 30.

The GPIB exists due to the need for a standard to control and communicate with multiple bench-top instruments. It also provides fast data transfer rates. GPIB is also relatively easy to program, enabling the communication to be readily established.

5.4.3 Programming

We have used LabVIEW as a programming tool to develop VIs for laser diode characterization. LabVIEW stands for 'laboratory virtual instrument engineering workbench'. It is an intuitive graphical programming language for engineers and

scientists and uses icons instead of lines of text to create applications. In contrast to text-based programming languages where instructions determine program execution, LabVIEW uses dataflow programming where the flow of data determines execution. LabVIEW is a powerful software tool for designing test, measurement & control systems as it provides complete integrated environment to interface with real-world signals, analyze data for meaningful information and display results in flexible manner. The LabVIEW contains high-level, application specific development tools and libraries with built-in data processing, data analysis and storage functions.

LabVIEW programs are called virtual-instruments, or VIs, because their appearance and operation imitate physical instruments. A VI consists of three components:

- Front panel - Serves as the user interface.
- Block diagram - Contains the graphical source code that defines the functionality of the VI.
- Icon and connector pane - Identifies the VI so that one can use the VI in another VI. A VI within another VI is called a sub-VI. A sub-VI corresponds to a subroutine in text-based programming languages.

The front panel is a set of controls for the user to manipulate while the system is running, whereas the block diagram is a collection of actions bound together like a flowchart. The front panel can be customized for any look and feel desired, thus preparing a graphical user interface (GUI), while the block diagram can be manipulated to clearly show the flow of data. The front panel of a LabVIEW VI contains controls and indicators. As their name suggests, controls are the inputs into the system, and the indicators are the outputs. In addition to the buttons and numeric indicators, an assortment of graphical displays, lights, meters, sliders, and other controls and indicators found on traditional instruments such as function generators and oscilloscopes can be used on the VI front panel to make the system interactive and easy to use.

The block diagram is where the user can link all the controls and indicators together with various logics and operations. Initially the user places the function icons that correspond to the actions they wish the system to take on the block diagram. They are

then "wired" together in a set order to produce a coherent path through the system. LabVIEW follows a dataflow model for running VIs. A block diagram node executes when all its inputs are available. When a node completes execution, it supplies data to its output terminals and passes the output data to the next node in the dataflow path.

Although the original use of LabVIEW was graphical measurement and data acquisition, it can also be used for general purpose programming. All of the basic functions of a traditional text-based language such as file input and output, data structures, and program flow are available in LabVIEW.

5.5 Experimental Setups and VI Implementations

5.5.1 L-I-V Characteristics and Spectral Response Measurement

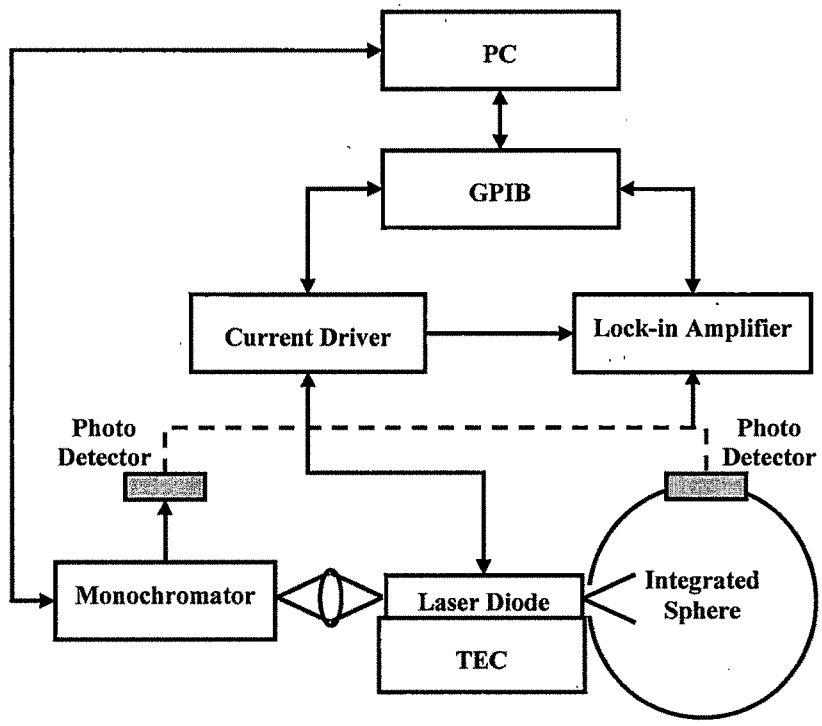

Figure 5.17: Block diagram of experimental setup for laser diode characterization.

Figure 5.17 shows the block diagram of experimental setup for laser diode characterization [19]. A high-power (65 A) laser diode current-driver (Newport-5600) and a low-power (3 A) precision pulsed current-driver (ILX-Lightwave LDP-

3840) have been used to drive current in the laser diodes depending on the laser diode structure. The optical power is measured using Newport's integrating sphere and Lock-in amplifier (SR-530). The current driver and Lock-in amplifier have been interfaced with PC using PCI-GPIB (IEEE-488.2). For spectral response, a monochromator (CVI-CM110) has been interfaced using serial port (RS232). These instruments are controlled by a VI made in LabVIEW 7.1. The actual photograph of L-I/I-V measurements setup is shown in figure 5.18.

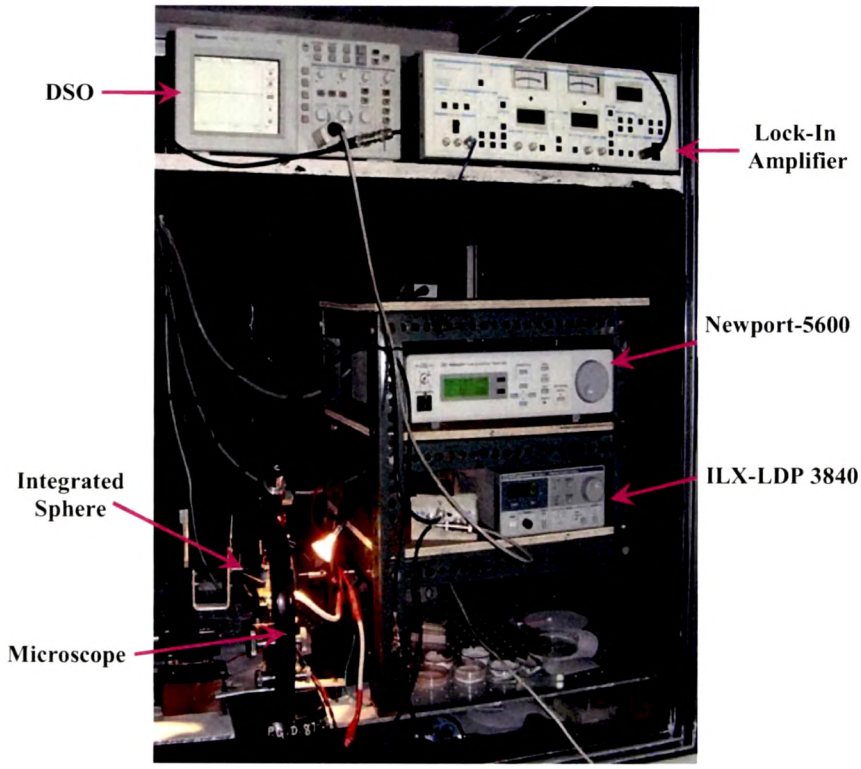

Figure 5.18: L-I/I-V characteristics measurement setup.

The laser diode bar is mounted on a TEC module and an individual laser diode stripe is probed using Gold coated Tungsten Carbide tip as shown in figure 5.19. TEC module is arranged on a heat sink with a DC fan. The probing is assisted by an XYZ mount as shown in figure 5.18.

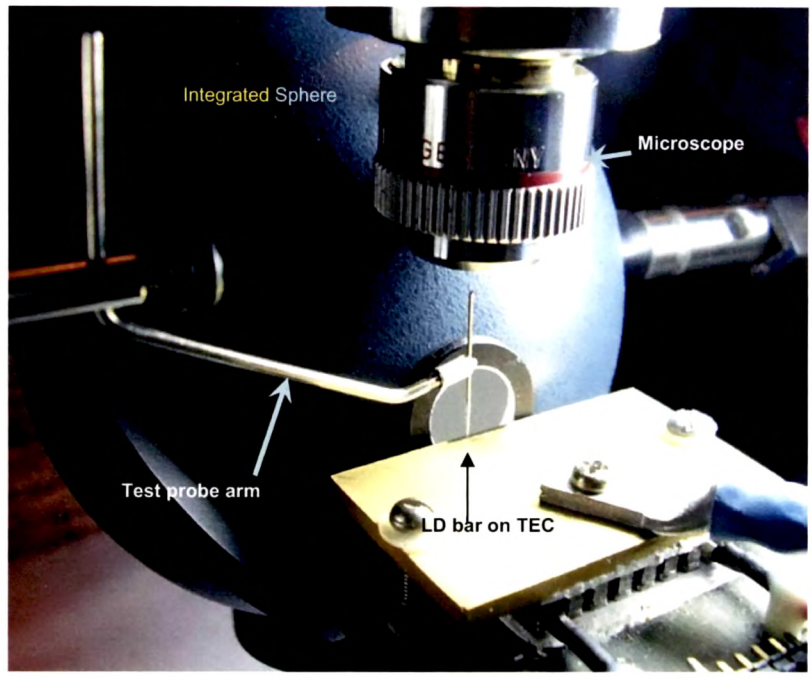

Figure 5.19 Laser diode probing for L-I/I-V characteristics measurements.

In case of spectral response, the light from laser diode is made to focus at the input of the Monochromator. The Monochromator wavelength is controlled by the VI. Again the output of Monochromator is fed to the photo detector through an optical chopper. This chopper provides the triggering to the Lock-in amplifier. Pictures of this setup are shown in figure 5.20 [a] and 5.20 [b].

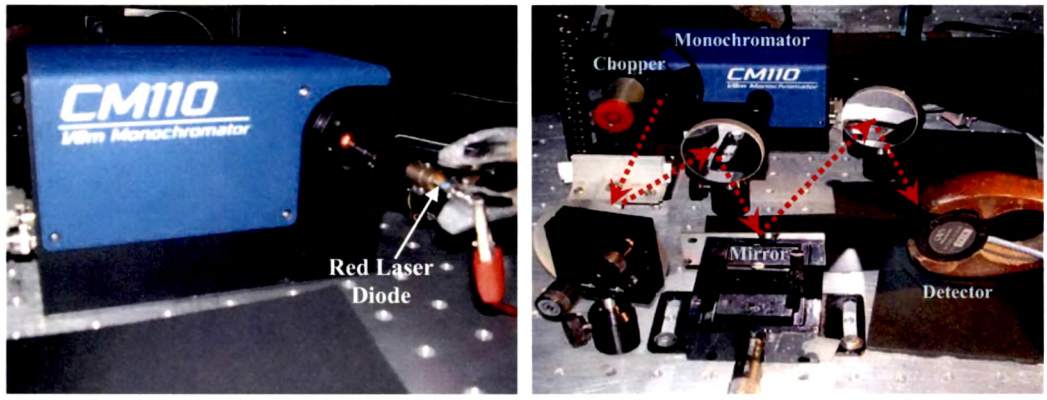

[a] **[b]**

Figure 5.20: Spectral response measurement setup.

A LabVIEW program, called virtual instrument (VI), measures either L-I and I-V Characteristics simultaneously or spectral response of the laser diode at a time. Features of the program include selection of current driver modes viz. I_o (Constant output current), I_m (Constant monitor photodiode current) and P_o (constant optical power), input current range, increment steps, time delay between two steps, Lock-in amplifier sensitivity, and data storage. User can also choose to operate the current driver in CW or QCW (pulsed) mode. In case of spectral response, the program provides control over monochromator grating selection, wavelength range, scanning steps and delay.

The L-I/I-V characteristics is separated from spectral response measurement using "Tab Control". In both the cases, the VI initializes respective instruments and checks for their status. For L-I/I-V Characteristics, the VI controls the current output of the driver using GPIB IEEE 488.2 commands. The light emitted by Laser Diode is collected by integrated sphere and corresponding photocurrent, generated by photodiode is measured using Lock-in amplifier whose output is read by the VI. The optical power and laser voltage are dynamically plotted against the input current. The linear portion of L-I and I-V curves are separated using the double differentiation of L-I and I-V curves. The post threshold portion is then fitted using "Linear Curve Fit" to get the slope and intercept. The Differential Quantum Efficiency of laser diode is obtained from the slope of linear portion of the L-I curve. However, the optical power obtained from L-I curve is the power emitted by the front facet. To calculate the differential efficiency, the total power generated inside the cavity is used, which is calculated from front facet output using known values of front and back facet reflectivities. The slop of the I-V curve gives the series resistance of laser diode.

In addition to the dynamic data acquisition and display, the program also analyzes the data and computes important parameters like lasing wavelength, threshold current, turn-on voltage and differential quantum efficiency for the laser diode. The results are displayed graphically as well as numerically. The programming code of the VI for laser diode characterization is shown in figure 5.21 [a]. Figure 5.21 [b] shows controls and indicators of graphical user interface (GUI) for the L-I/I-V characteristic measurement. The L-I curve plot on the GUI is shown in figure 5.21 [c]. GUI controls and plot of spectral response measurement of laser diode is shown in figure 5.21 [d].

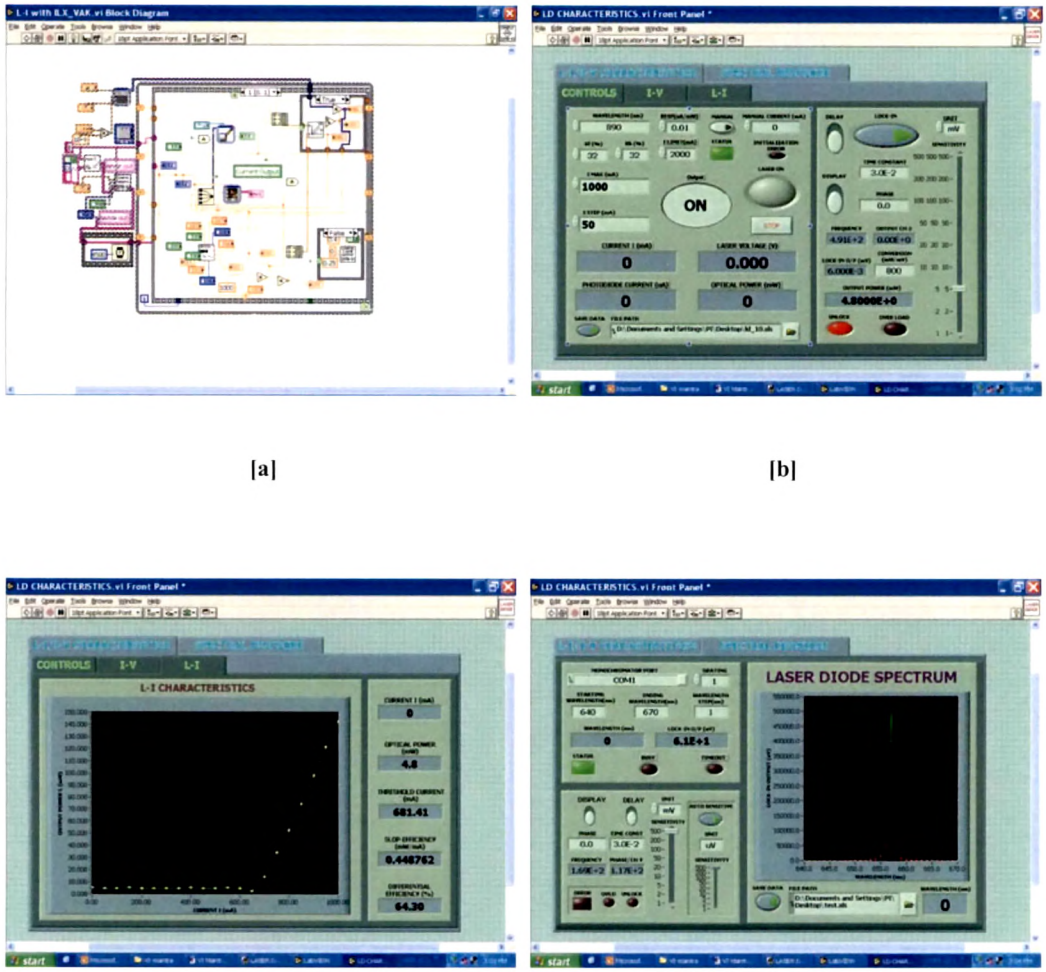

Figure 5.21: [a] Block diagram of VI and GUI Screen Shot for [b] controls of L-I and I-V characteristics [c] L-I characteristics plot and [d] Spectral response measurement.

The VI also analyzes the data, thus acquired in both the cases, and computes the important laser diode parameters. The overview of VI operation is given in the flowchart as shown in figure 5.22.

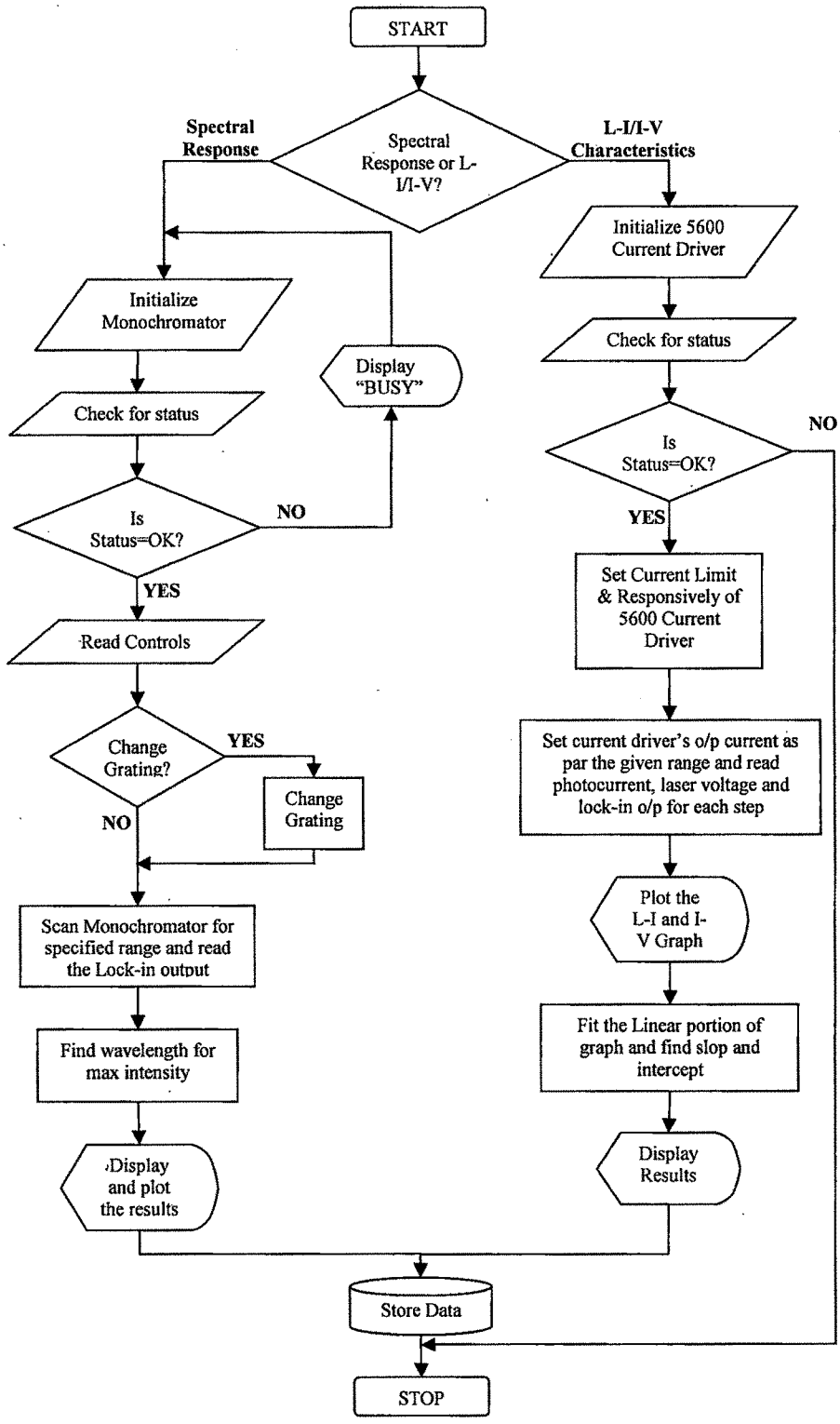

Figure 5.22: Flowchart explaining the VI operation.

We have carried out measurements of L-I/I-V characteristics and spectral response on different types of laser diodes using this automated setup. Types of laser diodes used for the experiments include InGaAlP quantum-well (QW) laser diodes lasing at 657 nm,

LPE grown AlGaAs based Separately Confined Heterostructures laser diodes lasing at 820 nm [20,21], GaAs QW laser diodes with 850 nm lasing wavelength, $Al_{0.3}Ga_{0.7}As/GaAs/Al_{0.3}Ga_{0.7}As$ Double-Heterostructure laser diodes lasing at 890 nm, and highly-strained InGaAs QW laser diodes grown by MOVPE with lasing wavelength of 1200 nm [22,23]. We have also carried out analytical simulation of L-I characteristics for different laser diode structures using LabVIEW [23].

Figure 5.23 [a] shows the experimental and simulated L-I Characteristics of 890nm laser diode. The spectral response of 657 nm (red) laser diode is shown in figure 5.23 [b]. The diode emission, in this case, was recorded from 640 nm to 670 nm with 1 nm step size and 2 nm band-pass of the monochromator.

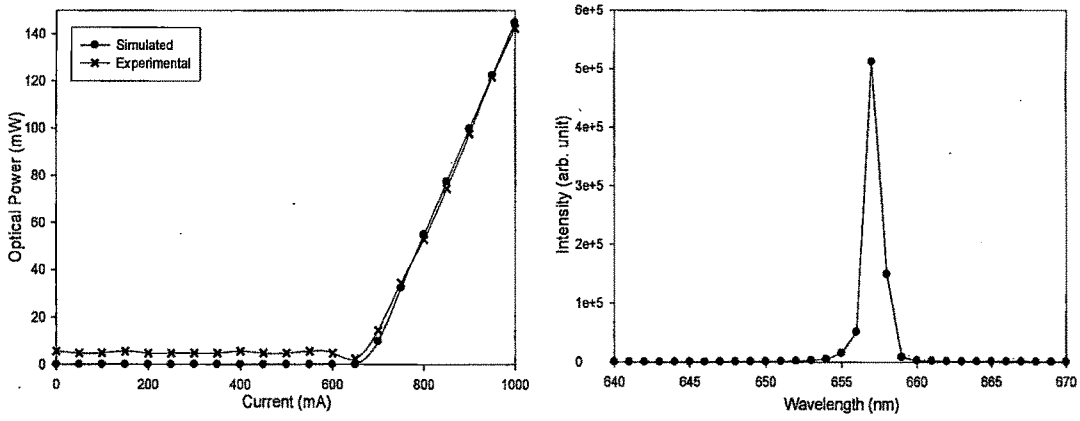

Figure 5.23: [a] Experimental and simulated L-I Characteristics of 890 nm laser diode, [b] spectral response of 657 nm (red) laser diode.

The experimental characteristics and extracted parameters are in very good agreement with the simulated results. The VI allows the user to carry out three main characterization of Laser diode in a same program. Thus, it is very useful in the field of research and other areas where frequent characterization of laser diode is required. Beside its obvious advantages over manual measurements like less time and effort consumption, the automated setup has many beneficial features including precision, consistency and uniformity in data acquisition, especially because these measurements have to be carried out in the dark room. Accuracy of L-I measurements is better than ± 2% mainly decided by the photodiode whereas the wavelength accuracy is ± 0.2 nm.

The limitation of this setup lies in the hardware side. As Newport's 5600 current driver is typically a high-power laser diode driver, it can not measure the voltage for low power laser diode below 1.5 V. More over, in the pulse mode, the duty cycle and frequency can not be controlled by the program. Similarly the minimum scanning step for spectral response is limited by the resolution of Monochromator.

Further, slight modification in the VI with required change in measurement conditions of experimental setup allows determination of more laser diode parameters as discussed earlier. Experimental setups and necessary modifications in VIs for measurements of parameters like Characteristic temperature T_0, Thermal Impedance R_{th}, degradation rate and life time of laser diodes are described here.

5.5.2 Characteristic Temperature Measurement

In most applications the ability of the laser diode to perform well at elevated temperatures is of great interest. The temperature of laser diode increases due to the self-heating or ambient temperature elevation of semiconductor crystal. Lattice heat is generated whenever physical processes transfer energy to the crystal lattice. This is especially of concern in the case of high-power laser diodes where the amount of heat generated causes the device temperature to rise significantly. As a result, it is of utmost importance for the semiconductor crystal to be robust enough so as not to degrade due to device operation at high temperatures. The characteristic temperature, T_0, is a measure of the temperature sensitivity of the laser diode [24]. Higher value of T_0 indicates that the threshold current density and the efficiency of the laser diode are less sensitive to the temperature and thus, the laser diode is thermally more stable. We have determined the characteristic temperature from its dependence on threshold current.

The threshold current of laser diode increases with temperature in all types of semiconductor laser because of various complex temperature dependent factors. The complexity of these factors prevents the formulation of single equation holding for all devices and temperature ranges. However, the variation of threshold current with temperature can be approximated by the empirical expression [25],

$$I_{th} = I_0 \exp\left(\frac{T}{T_0}\right) \tag{5.2}$$

Here, I_{th} is the threshold current, I_0 is a constant, T is the operating temperature and T_0 is the characteristic temperature of the laser diode. Modifying equation 5.2, we get,

$$\ln(I_{th}) = \frac{T}{T_0} + \ln(I_0) \tag{5.3}$$

Plotting $\ln(I_{th})$ versus operating temperature T gives a straight line whose slop gives the inverse of characteristic temperature T_0.

Thus, in order to measure the characteristic temperature of a laser diode, we have experimentally measured the L-I curve of a laser diode at different operating temperatures. The L-I characteristics were measured in pulsed mode at vary low duty-cycle, typically 0.25%, to avoid self heating of the device. Hence we can assume that the laser diode chip is at the same temperature as that of the base on which it is mounted. We varied the temperature of the mount from 10 to 60 °C. The VI is modified to control and maintain the temperature by means of TEC power and take the L-I characteristics measurements in given range of temperatures at given temperature increment steps. We could not go below 10 °C because operating a laser, which is not hermetically sealed, at temperature significantly lower than the room temperature results in water condensation on the device causing damage to the laser diode due to electrical shorts. The characteristic temperature of the device is determined from these experimentally measured L-I curves by plotting the threshold current I_{th} versus the temperature on a logarithmic scale and then measuring the slope of the linear fit line.

5.5.3 Thermal Impedance Measurement

The efficient heat removal from the junction of a semiconductor laser is all important for high-power performance. The efficiency of heat removal is usually expressed as R_{th} which is defined as [26],

$$R_{th} = \frac{\Delta T}{\Delta P} \tag{5.4}$$

where ΔT is the difference between temperature of the junction (active-region) and that of the heat sink and ΔP is the power dissipated within the device.

The thermal impedance is an important parameter for a semiconductor laser, especially for high-power laser diodes where a high current is used to drive the laser to achieve a required performance. Higher the thermal impedance of the device, poorer is the heat removal and consequently higher the temperature of active region resulting in fast degradation of the device.

Measurement of the thermal impedance of a laser diode involves determining the temperature difference between the active region and the heat sink produced by a known dissipation of the input power. However, it is difficult to measure the active region temperature directly. The temperature changes may be deduced from various optoelectronic parameters which are sensitive to the temperature of the active region. These parameters involve the wavelength of the longitudinal modes and peak of the emission spectrum, the lasing threshold current, the terminal voltage and emitted optical power. To obtain the temperature difference, the laser diode is operated in both pulsed and CW mode and the value of any of the above mentioned temperature dependent parameters of the laser diode in pulsed operation is compared with that obtained in the CW operation. Here, it is assumed that the heat generated in pulsed mode with very low duty-cycle is negligible and the temperature of the active region is same as that of the heat sink.

To determine the thermal impedance from terminal voltage, emitted optical power and longitudinal made wavelength null technique is used. In this technique, the CW heating of the active region was compensated by the reduction in heat sink temperature necessary to return the CW value of the specified parameter to the pulsed value at the same current [26]. We have used temperature dependence of threshold current of laser diode to measure the thermal impedance. Typical L-I characteristics in pulsed and CW mode are given in figure 5.24.

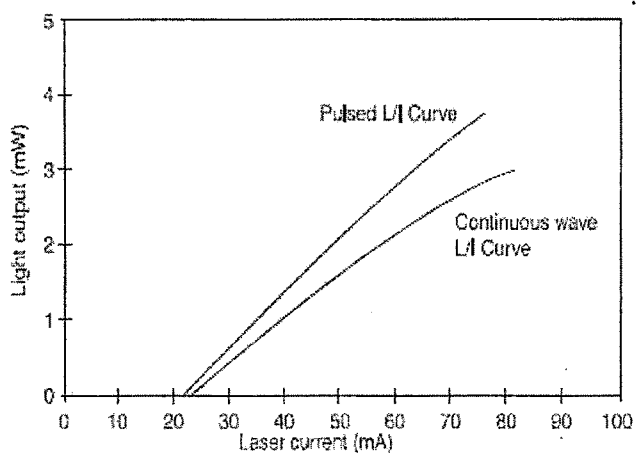

Figure 5.24: Comparison of L-I characteristics of a laser diode in CW and pulsed mode.

From equation 5.3, we can write,

$$T = T_0 \ln\left[\frac{I_{th}}{I_0}\right] \tag{5.5}$$

And therefore,

$$\Delta T = T_0 \ln\left[\frac{I_{th}(CW)}{I_{th}(Pulsed)}\right] \tag{5.6}$$

Then using the known difference in power injected in to the laser between the pulsed and CW operation, one can calculate the thermal impedance by the formula [27],

$$R_{th} = \frac{\Delta T}{\Delta P} = \frac{T_0 \ln[I_{th}(CW)/I_{th}(pulsed)]}{[V_{th}(CW)\times I_{th}(CW) - OP(CW)]} \tag{5.7}$$

where, $I_{th}(CW)$ is the threshold current in CW mode, $V_{th}(CW)$ is the voltage across the laser diode at threshold in CW, $I_{th}(pulsed)$ is the threshold current in the pulsed mode, $OP(CW)$ is the optical power at threshold in CW mode, T_0 is the characteristic temperature of the laser diode obtained by method described in previous section.

The experimental setup for thermal impedance measurement does not use constant current driver and lock-in amplifier. This is because the current driver LDP-3840 does not

provide CW mode operation and Newport-5600 can not be used for very low current applications, since it is meant for high-power operation only. Alternatively, we used PCI-6024E DAQ card along with BNC 2120, and a voltage follower (buffer) circuit to drive the CW current and measure optical power and voltage drop across the laser diode. The voltage follower between BNC 2120 and laser diode is used to increase the current capacity as the current capacity of BNC 2120 is very low. The voltage follower also provides isolation between the computer and laser diode circuitry. The block diagram of the new setup is shown in figure 5.25.

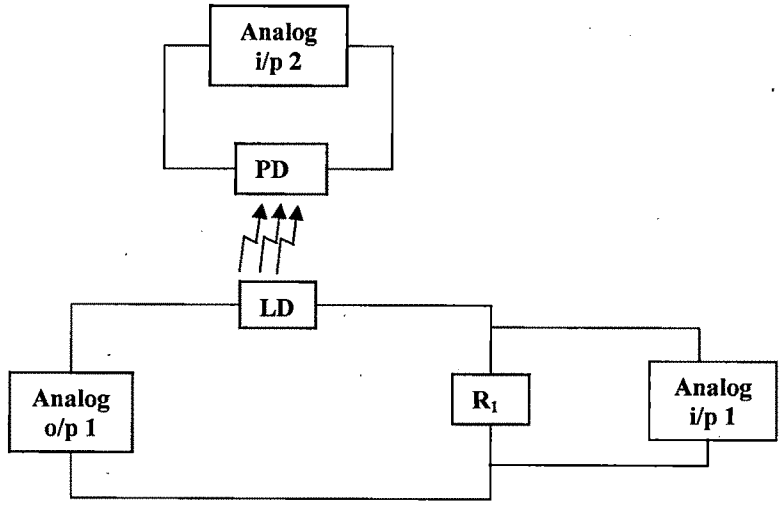

Figure 5.25: Block diagram for thermal impedance measurement of laser diode.

The LabVIEW program is modified to measure both pulsed and CW measurements using the new setup. Since the DAQ card can not supply constant current, the current in the circuit is controlled programmatically by monitoring the current flowing through the circuit and controlling the output voltage of AO-1 channel of BNC-2120. The DAQ card can not even read the current directly. A small series resistance of known value R_I is used to monitor the current as shown in figure 5.25. The voltage drop across the resistance is read by channel AI-1. Channel AI-2 is used to read the optical power by means of photo-voltage of the photodetector. Just in a single run, the program takes L-I and I-V characteristics in both pulsed and CW measurements and calculates and display the thermal impedance using equation 5.7.

This experiment is very useful to find the thermal impedance of various laser diode bars with different structures and can be a very important tool for testing and characterization of die-bonding and packaging processes for high-power laser diodes.

5.5.4 Lifetime and Degradation Rate Measurement

Reliability is a concern in every laser diode application. In general, laser diode reliability may be defined as the ability to operate the device satisfactorily in a defined environment for a specified period of time. Laser diode suffers various degradation processes during its lifetime as discussed in chapter 4. Laser diode life testing is used for part qualification during product development as well as for lot testing throughout the production life of the laser. Life tests generally consist of monitoring the operation of a sample group of lasers under carefully controlled conditions. Degradation is observed and recorded throughout the test by precise measurement of changes in the laser's operating characteristics.

There are several methods of extrapolating source lifetime. Depending on the type and application of the laser diode, life test studies involve the periodic measurement of a variety of device parameters including operating current, optical output power, threshold current, and forward voltage. Aging studies are conducted in one of the following modes of operation:

- Constant Current Aging

Constant current aging mode is often referred to as ACC (automatic current control) mode [28]. In this mode laser current is held constant for the duration of the test and the optical output power is monitored continuously. The optical power shows exponential decay with time at constant current, following equation 5.8, due to the device degradation [29].

$$P_{out}(t) = P_0 \exp\left(-\frac{t}{\tau}\right) \tag{5.8}$$

Here, P_0 is the initial power output of the device at time t=0 and τ is the exponential lifetime. The lifetime of the device can be determined by plotting the optical power data obtained for a long time t and fitting the curve with exponential decay curve.

➢ Constant Power Aging

Constant power aging mode is also referred to as APC (automatic power control) mode [28]. In this mode, laser output power is held constant by continuously adjusting current. The operating current has to be increased to maintain the constant optical power from the laser diode due to the device degradation. Conventionally, the laser diode lifetime is defined at the 50% increase of operating current (Iop) [30]. Thus, by plotting operating current as a function of time, we can extrapolate the time necessary to increase the current by 50% of initial current for constant optical power and can determine the life time of the device. Constant power aging is used most frequently in life test studies because it closely resembles the typical mode of operation of laser diodes in use.

To reduce the testing time, often the life time of laser diode is measured with the help of accelerated aging by performing the experiment at precisely controlled high temperature. Aging is empirically related to temperature through the Arrhenius equation:

$$t = c\exp\left(\frac{E_a}{kT}\right) \tag{5.9}$$

where, c is a device constant in units of time, E_a is the activation energy, and k and T are Boltzman's constant and absolute temperature respectively. Depending on the type of laser, typical activation energies range from 0.2 eV to 0.7 eV [28].

Thus, to measure the life time τ_1 of the laser diode at room temperature T_1, the experiment is performed at high temperature T_2 and the life time at that temperature τ_2 is obtained. Then by using equation 5.9, one can get the life time at room temperature as,

$$\tau_1 = \tau_2 \exp\left[\frac{E_a}{k}\left(\frac{1}{T_1} - \frac{1}{T_2}\right)\right] \tag{5.10}$$

We have developed the VI using LabVIEW that allows the life time measurement in both ACC and APC mode. The user can chose the measurement mode from the front panel. Moreover, for accelerated aging, the experiment can be carried out at higher temperature. The VI controls the temperature using a TEC. The experimental setup is again somewhat similar to that of thermal impedance measurement. The current is

supplied to the laser diode programmatically using PCI-6024E DAQ card through BNC-2120 and a buffer. Channel AO-1 is used for this purpose. The current is monitored using a small resistance of known value R1. The voltage across R1 is read by channel AI-3. The voltage across the laser diode is also monitored continuously using channel AI-4. The light from the laser diode is made to fall perpendicular on to the photodetector. The photo-voltage from the detector is measured with the help of channel AI-5. The VI records and displays the current, the voltage across the laser diode and the optical power at the desired interval of time. In ACC mode, the VI maintains the constant current programmatically while in APC mode, the VI supplies the current necessary to maintain constant optical power. The laser diode and the photodetector both are kept at constant temperature using a TEC to avoid temperature instability during the experiment. The experiment is carried out in a dark box to avoid effects of other light sources. The whole experiment is provided with the UPS backup system in order to avoid problems of electrical power failures during the experiment which runs for a few days. Further, Laser diode life test studies require the accurate measurement of changes in laser operating parameters as small as a few percent over thousands of hours. Consequently, the stability of the measurement equipment must be very high, typically on the order of 0.1% per 1000 hours. The DAQ card PCI-6024E provides the stability of 0.01% per 1000 hours.

In ACC mode, when user stops the experiment, the VI plots the optical power over the complete experiment time and the power versus time curve is fit to the exponential decay curve of the type

$$y = A\exp[-Bx] \tag{5.11}$$

Thus, from equation 5.8, we get the life time of the laser diode as

$$\tau = \frac{1}{B} \tag{5.12}$$

The final result of life time is displayed on the front panel and recorded in the file along with the sample details and measurement mode.

In APC mode, the operating current is plotted against the whole experiment time on pressing the 'Stop' button. The VI then fits the data with the best fit curve and extrapolates the curve to find the time for 50% increment in the operating current. The

results are again displayed on the front panel as well as stored in a file along with sample details and the measurement mode.

The front panel and the block diagram of the VI are shown in figure 5.26 [a] and 5.26 [b] respectively.

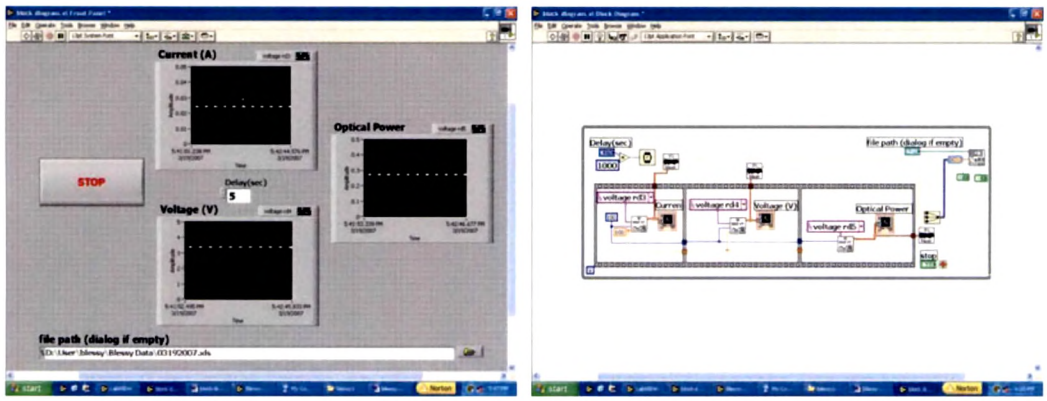

[a] [b]

Figure 5.26: [a] Front panel and [b] block diagram of the laser diode life-time measurement VI.

In both the modes, if the experiment is carried out at higher temperature for accelerated aging, the VI also takes the temperature in to the account while performing the final calculation and finds the life time of the laser diode at the room temperature using equation 5.10.

➢ References

[1] Pallab Bhattacharya, "*Semiconductor Optoelectronic Devices*", pp. 267, Prentice-Hall, India, (1999)

[2] Tyll Hertsens, "*Measuring Diode Laser Characteristics*", ILX Lightwave-Application note-**5**: An overview of laser diode characteristics, (2000)

[3] Peter Unger, "*Introduction to power diode lasers*", High Power Diode Lasers, Ed.: R. Diehl, *Topics Appl. Phys.*, **78**, pp. 31, Springer-Verlag Berlin Heidelberg, (2000)

[4] H. Kressel, J. K. Butler, "*Semiconductor Lasers and Heterojunction LEDs*", pp. 478, Academic Press, New York, (1977)

[5] Berthold E. Schmidt, Stefan Mohrdiek, Christoph Harder, "Pump Laser Diode", Optical Fiber Telecommunications IV-A, Ed.: Ivan P. Kaminow, Tingye Li, pp. 572, Academic Press, (2002)

[6] Mool Chand Gupta and John Ballato, Ed.; "Hand-book of Photonics", 2nd Edn., pp. 9-4, CRC Press, (2006)

[7] S. M. Sze, "*Physics of Semiconductor Devices*", pp. 733, Wiley-Interscience, New York, (1969)

[8] Y. Nakano, Y. Ushida, K. Tada, *IEEE Photon. Tech. Lett.*, **04(04)**, pp. 308, (1992)

[9] D. A. Yanson, E. U. Rafailov, G. S. Sokolovskii, V. I. Kuchinskii, *J. Appl. Phys.*, **95(3)**, pp. 1502, (2004)

[10] Toshio Higashi, Tsuyoshi Yamamoto, Shouichi Ogita, Masahiro Kobayashi, *IEEE J. Quant. Electron.*, **34(9)**, pp. 1680, (1998)

[11] Peter Blixt, John E. Bowers, Erik Bodtker, O. Sahlen, Roy S. Smith, *IEEE Transact. on Microwave Theory and Tech.*, **43(9)**, pp. 2214, (1995)

[12] Hiroshi Hatakeyama, Koji Kudo, Yoshitaka Yokoyama, Koichi Naniwae, Tatsuya Sasaki, *IEEE J. Sel. Topics Quantum Electron*, **8(6)**, pp. 1341, (2002)

[13] Scott T. McCain, Michael E. Gehm, Yanqia Wang, Nikos P. Pitsianis, Michael E. Sullivan and David J. Brady, Proc. of SPIE, 5864, OSA Biomedical Optics, Novel Optical Instrumentation for Biomedical Applications II, Eds.: Christian D. Depeursinge, (2005)

[14] N. Beverini, G. Del Gobbo, G. L. Genovesi, F. Maccarrone, F. Strumia, F. Paganucci, A. Turco, M. Andrenucci, *IEEE J. Quant. Electron.*, 32(11), pp. 1874, (1996)

[15] Xinlu Zhang, Yuezhu Wang, Youlun Ju, *Journal of Optics and Laser Technology*, **39(1)**, pp. 78, (2007)

[16] D P Blair, P H Sydenham, *J. Phys. E: Sci. Instrum.*, **8**, pp. 621, (1975)

[17] M. Santori, *IEEE Spectrum*, **27(8)**, pp. 36, (1990)

[18] "*GPIB 101 - A Tutorial About the GPIB Bus*", Application Bulletin AB48-11, ICS ELECTRONICS-IEEE 488, (2006)

[19] V. A. Kheraj, P. K. Patel, C. J. Panchal, T. K. Sharma, *Proc. of Sixth DAE-BRNS National Laser Symposium (NLS-6)*, Indore, India, pp. 70, (2006)

[20] S. S. Chandvankar, A. P. Shah, A. Bhattacharya, K. S. Chandrasekaran, B. M. Arora, *J. Cryst. Growth*, **260**, pp. 348, (2004)

[21] C.J. Panchal, K.M. Patel, V.A. Kheraj, S.S. Chandvavkar, A.P. Shah, A. Bhattacharya, B.M. Arora, *Proc. of Fourth DAE-BRNS National Laser Symposium (NLS-4)*, Mumbai, India, pp. 128, (2005)

[22] T. K. Sharma, M. Zorn, F. Bugge, R. Hulsewede, G. Erbert, M. Weyers, *IEEE Photon. Tech. Lett.*, **14(7)**, 887, (2002)

[23] V. A. Kheraj, C. J. Panchal, P. K. Patel, B. M. Arora, T. K. Sharma, *Journal of Optics and Laser Technology*, **39(7)**, pp. 1395, (2007)

[24] Bernd Witzigmann, Mark S. Hybertsen, *IEEE J. Sel. Topics Quantum Electron*, **9(3)**, pp. 807, (2003)

[25] S. M. Sze, "*Physics of Semiconductor Devices*", pp. 731, Wiley-Interscience, New York, (1969)

[26] Joanne S. Manning, *J. Appl. Phys.*, 52(5), pp. 3179, (1981)

[27] T.V.S.L. Satyavani, Deepti Jain, Amit Bhatti, S.K. Mehta, H.P. Vyas, *Proc. of Sixth DAE-BRNS National Laser Symposium (NLS-6)*, Indore, India, pp. 68, (2006)

[28] Johnson, L.A., *IEEE Communications Magazine,* **44(2)**, pp. 4, (2006)

[29] Melanie Ott, "*Capabilites and Reliability of LEDs and Laser Diodes*", Report no. 301-286-0127, NASA Goddard Space Flight Center

[30] Nam Hwang, Min-Kyu Song, Seung-Goo Kang, Hee-Tae Lee, Kyung-Hyun Park, Dong-Boon Jang, Seong-Su Park, Hak-Soo Han, Dong-Goo Kim, and Hyung-Moo Park, *IEEE Proc. 45th Electronic Components and Technology Conference*, pp. 318, (1995)